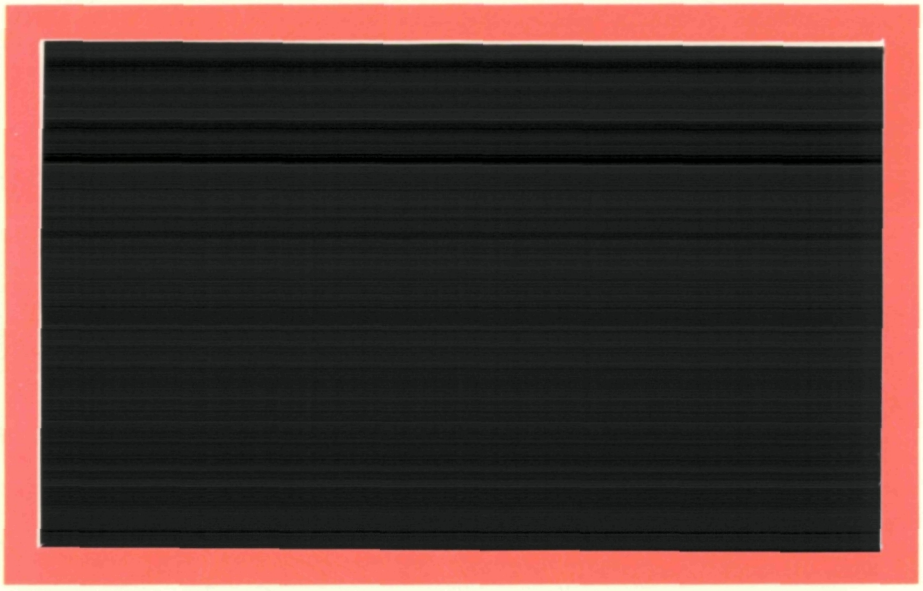

(NASA-CR-189883) PROTEIN CRYSTAL GROWTH IN LOW GRAVITY Semiannual Technical Report, 6 Jun. - 6 Dec. 1991 (Stanford Univ.) 25 p
CSCL 22A
G3/29
N92-18247
Unclas
0070325

CENTER FOR MATERIALS RESEARCH

STANFORD UNIVERSITY • STANFORD, CALIFORNIA

The Board of Trustees of the
Leland Stanford Junior University
Center for Materials Research
Stanford, California 94305-4045
Santa Clara, 12th Congressional District

Semi-Annual Technical Report
on
PROTEIN CRYSTAL GROWTH IN LOW GRAVITY
NASA #NAG8-774
CMR-92-1
SPO#7218
for the period
June 6, 1991 through December 6, 1991

Submitted to
George C. Marshall Space Flight Center
ES-76, Space Science Lab
MSFC, AL 35812

Principal Investigator:

Robert S. Feigelson, Professor (Res.)
Center for Materials Research
Stanford, California 94305-4045
(415) 723-4007

February 1992

TABLE OF CONTENTS

ABSTRACT

This report covers the period of June 6, 1991 to December 6,1991 for NASA Grant NAG 8-774. The objectives of and approach to the research is outlined. A study of the crystallization of isocitrate lyase (ICL) is presented and the influence of the lack of thermal-solutal convection in μg on the morphology of ICL crystals is discussed. The latest results of studies with thermonucleation are presented. These include the nucleation of a protein with retrograde solubility and an unknown solubility curve. A new design for a more μg compatable thermonucleator is presented.

I. INTRODUCTION

The objective of this research is to study the effect of low gravity on the growth of protein crystals and those parameters which will affect growth and crystal quality. The proper design of the flight hardware and experimental protocols are highly dependent on understanding the factors which influence the nucleation and growth of crystals of biological macromolecules. Thus, the primary objective of this research is centered on investigating those factors and relating them to the body of knowledge which has been built up for "small molecule" crystallization. This data also provides a basis of comparison for the results obtained from low-g experiments.

The main component of this research program is the study of mechanisms involved in protein crystallization and those parameters which influence the growth process and crystalline perfection. Both canavalin and lysozyme are being used as the basic model proteins in these studies. Other biological macromolecules such as isocitrate lyase have been included in this research program when they provide an opportunity to better understand the nature of the crystallization process. The program involves four broad areas:

1. The application of both classical and novel chemical and physical techniques to study the fundamentals of protein crystallization. Included in this area are the study of the phase relationships in the systems of interest, primarily the factors controlling solubility, the study of growth kinetics to determine the growth rate controlling mechanism and the relevant activation energy involved in the process.

The effects of fluid flow on the growth and perfection of protein crystals will be studied using flow visualization techniques. The use of electrochemical techniques to monitor and/or control crystallization will be studied also. The effects of applied voltages on nucleation and growth are not known nor is the magnitude of the potentials which may develop on the crystal during growth.

2. Characterization of protein crystals. Optical microscopy will give a general evaluation of crystal morphology, size and perfection. Phase contrast techniques will give enhanced contrast to the surface features allowing observation down to the 0.1μ level. For more detailed surface imaging the application of Scanning Tunneling Microscopy and Atomic Force Microscopy to protein crystals will be investigated. To study the defects occurring in the bulk of the crystals, the applicability of Synchrotron x-ray topography will be studied. The characterization studies will be attempting to associate the defects in protein crystals with the growth conditions to develop insights for growing crystals of greater perfection.

3. Control of nucleation and growth. The information developed in the phase relationship studies of section (1) will be used to design experiments to separately control the nucleation and growth processes. The information from section (2) will be used to optimize the growth.

4. The design and construction of a prototype of space flight hardware. The design will incorporate the results of section (3) and will be instrumented to gather the types of data that have been acquired in the ground based studies.

II. ISOCITRATE LYASE

The structure of the protein isocitrate lyase (ICL) has been under study for a number of years at Du Pont Merck. Attempts to grow isocitrate lyase crystals by the hanging drop method produced crystals with very poor growth morphologies (Fig. 1). It was not immediately clear whether this poor morphology was due to unstable growth conditions or sedimentation. A series of experiments were designed to answer this question. In addition to the ground based experiments, ICL has been flown as part of the NASA shuttle program. As a result of these experiments and the application of theoretical evaporation models to the crystallizing system, factors affecting the growth of ICL crystals and, by extension, other protein crystals became apparent.

All of the ICL used in these experiments came from Du Pont Merck. Before use, the ICL solution (ICL in 0.1M Tris-HCl pH 7.8, 10mM EDTA, 1mM DTT, 0.4M KCl) was incubated at 4°C for 24 hrs with a reducing solution (0.3M Glutathione, 66mM EDTA in 1M Tris-HCl pH 8.0) (4:100 v/v) and an inhibitor solution (50mM 3-nitriproprionate, 0.5M MgOAc in 50mM Tris-HCl pH 7.0) (4:100 v/v). The ICL concentrations were 10mg/ml (Du Pont Merck) and 12mg/ml (Stanford). The well solution was 1.6-2.0M (60-80% saturation) Na-citrate (Na-cit). The usual drop size was 4μl (2μl ICL solution and 2μl well solution). Crystals appeared within one week at 24°C.

The source of the poor morphology was investigated by closely observing drops during crystallization. These 4μl hanging drops (12mg/ml ICL solution, 72% Na-Cit well solution) were observed through a microscope at 150x.

Figure 2 shows a typical result of the 4μl hanging drop experiments. The crystal is more obviously dendritic than those grown from a 30μl drop (Fig. 1). It is obvious that the poor morphology resulted from uncontrolled growth originating at the corners of the crystal. Such growth can result from either excessive supersaturation[1] or from flow effects.[2] In an attempt to separate these effects, a glass schlieren imaging cell (1mm x 3mm rectangular cross section) was built and 4μl of ICL crystallizing solution was vapor equilibrated against Na-cit in the well of the cell. While no flows were observed, in this experiment, the three crystals were found growing in this cell had a more regular morphology than had been previously observed in the hanging drop experiments (Fig. 3).

The same growth experiment was repeated in circular cross section capillaries (1.88mm diameter) to better observe the crystals. The ICL crystals grown in these capillaries exhibited a very well formed morphology (Fig. 4). These crystals have been x-rayed and have the same space group ($P2_12_12_1$) and unit cell parameters (a=80.7Å, b=123.1Å, c=183.4Å) as the previously grown crystals. The "octagonal" cross section

arises from the orthorhombic symmetry with the facets bounded by (100), (010) and (110) faces. The end of the crystals are bounded by either (001) (flat) or (101) (wedge shaped) faces.

A comparison of Figs. 2 & 4 shows that the initial breakdown in morphology occurs at the corners of the crystal. This breakdown is probably associated with excessive supersaturation and, thus, with unstable growth conditions.

Sibille and his co-workers have developed mathematical models to describe the evaporation from both drops and capillaries in equilibrium with well solutions.[3,4] These models may be expressed in the general form as:

a) for the hanging drop

$$t / t = F[x(t)]$$

and b) for the capillary

$$t / t = G[\partial(t)]$$

where

$$x(t) = \frac{a(t)}{a_O}; V(t) = \Omega_v(\alpha)\, a(t)^3; \Omega_v(\alpha) = \frac{4}{3}\pi \cos^4(\tfrac{1}{2}\alpha)[\,1+2\sin^2(\tfrac{1}{2}\alpha)]$$

where a is the contact angle of the drop, and

$$\partial(t) = \frac{\Delta_1(t)}{\Delta_1(0)}; \Delta_1(t) = n_1(e)[t] - n_1(c)[t]$$

where $n_1(e)[t]$ is the number of moles of water in the crystallizing solution and $n_1(c)[t]$ the number of moles of water in the well. The characteristic times, t, for the two models are defined by:

a) for the hanging drop

$$\tau = \frac{3\,\Omega_v(\alpha)\, a_0^2\, n_1(b)\, R\, T}{\Omega_a(\alpha)\, D_1\, p_1^0\, w\, n_2(b)\, V_1}; \Omega_a(\alpha) = 4\pi\cos^2(\tfrac{1}{2}\alpha)$$

and b) for the capillary

$$\tau = \frac{R\, T\, L\, \Delta_1^{\,2}(0)}{4S\, D_1\, p_1^0\, w\, n_2}$$

where $n_1(b)$ is the number of moles of water in the well, D_1 the diffusion coefficient of water in air, p_1^0 the vapor pressure of pure water, w the vapor pressure lowering constant, $n_2(b)$ the number of moles of precipitant in the well, V_1 the partial molar volume of water, L the distance between the crystallizing solution and the well, S the cross sectional area of the capillary, n_2 the total number of moles of precipitant in the crystallizing solution and the well, and R and T have their usual meaning. The parameters needed to use these models for ICL and lysozyme were calculated as outlined in ref.[3] The osmotic coefficient for Na-cit was estimated using equation 10, section 14 of Shoemaker and Garland.[5] The contact

angle for the hanging drop simulations was 90°, the well volume 500µl and the spacing 5mm. The well volume for the capillary simulations was 350µl and the spacing was 3.5cm. Figure 5 compares the results of applying these models to a drop and a 1.88mm ID capillary containing the same volume of ICL solution. The drop evaporates at a rate which is two orders of magnitude faster than the capillary. This difference in rates is consistent with laboratory observations.

The rate of change of supersaturation is somewhat more complicated than the rate of change in volume of the crystallizing solution since the concentration of both the crystallizing species and the precipitant change with the change in volume and, through the solubility curve, both affect the supersaturation. The supersaturation is further affected by the growth of crystals in the solution. Unfortunately, neither the solubility curve nor the growth kinetics of ICL is known. In order to estimate how supersaturation would change during crystal growth by vapor equilibration, the models of Sibille et al [3,4] were applied to lysozyme crystallization using the solubility data reported by Pusey[6] and the growth kinetics described by Pusey and Naumann.[7] The growth solution modelled contained 30mg/ml lysozyme and 2% NaCl equilibrated against a well of 4% NaCl. Ten crystals were assumed to nucleate at c/s = 4 (a value consistent with other studies). No further nucleation was allowed to take place. The amount of lysozyme removed from solution during each growth period was determined. Figure 6 shows the results for both a hanging drop and a capillary. The supersaturation in the drop reaches a peak which is almost double that of the capillary. The crystallizing system can react to this increased supersaturation by either 1) nucleating more crystals (secondary nucleation), 2) increasing the growth rate to the point of instability or 3) a combination of the two. Lysozyme does the latter exhibiting secondary nucleation together with surface roughening. ICL ,on the other hand, exhibits morphological instability

Figure 7 shows an ICL crystal which was grown by Du Pont Merck in low-g during a shuttle mission. The morphology is greatly improved over those grown by the hanging drop technique on Earth. The drops used in space were larger (30µl vs. 4µl) than those used on Earth which raises the question of whether the improvements in crystal quality are related to the effects of µg or simply the difference in evaporation rate. Figure 8 shows the theoretical evaporation rates for 4µl and 30µl drops. The rate of equilibration was 5x slower for the larger drop, but the crystals shown in Figs. 1 & 2 were grown under the same conditions. While there was some improvement in the morphology of the 1-g crystal grown from a 30µl drop (Fig. 1), the decrease in equilibration rate can not satisfactorily explain the greatly improved morphology found in the ICL crystals grown in space from the same size drop.

There are other factors which may affect the morphology of space grown crystals. It has been pointed[3] out that drops evaporate slower than predicted in space due to the existence of a concentrated layer of precipitant near their surfaces which lowers the vapor pressure of the drop and retards evaporation. The preliminary data in ref.[3] indicated that the rate of evaporation decreased by a factor of about 2. This would produce a lower evaporation rate (10x) for 30μl drops in μg compared to 4μl drops at 1-g . This is still an order of magnitude faster than the equilibration rates for the capillary experiments. Clearly, the reduced equilibration rate due to the presence of a concentrated salt layer at the liquid-vapor interface was not the only factor contributing to the improved quality of the space grown ICL crystals.

In an attempt to simulate μg conditions on the ground and to provide a further basis for comparison between protein crystal growth at 1-g and μg, a series of capillary ICL crystal growth experiments were preformed together with some simulated growth experiments (identical solutions without protein). Experiments were conducted with the capillary in both the normal and inverted positions. In the latter case, it was hoped that gravity would stabilize the denser salt layer at the liquid-vapor interface. In the simulated growth experiments, the inverted capillaries equilibrated at a slightly slower rate. In the actual growth experiments, a precipitate layer appeared at the liquid-vapor interface in the inverted capillaries. No precipitate was found in the normal capillaries, nor did such layers appear in the simulated growth experiments and it must be concluded that the precipitate was isocitrate lyase. In some cases crystals eventually grew in this layer. The existence of the precipitate in the surface layer decreases the supersaturation in the ICL solution in the same manner as the growing crystals did in the lysozyme growth simulation. Therefore, the ICL crystals were actually growing from a lower supersaturation than would be expected on the basis of evaporation alone. If Sibille's model of the stable surface layer in μg[3] is correct, then this mechanism can explain the improved crystal morphology seen in the ICL μg experiments.

"Octagonal" ICL crystals were only observed in the normal capillary configuration. This configuration promotes solutal convection. The solute Rayleigh number based on a ICL crystallizing solution with a depth of 7.2mm is approximately $2x10^6$ which is in excess of the critical Rayleigh number for aqueous solutions of 300. Even correcting for the size of the capillary, the Rayleigh number would be as high as 10^4. The time for onset of convection calculated from the time dependent Rayleigh number was approximately $1x10^{-3}$ seconds. There will be mixing in this configuration and the results indicate that some degree of mixing is desirable in the growth of ICL from capillaries.

The poor morphology of the ICL crystals grown by the hanging drop method in 1-g was due to high (unstable) growth rates due to high supersaturation. While it is necessary in all unseeded "batch" type crystal growth to increase the supersaturation high enough to cause nucleation, a slower rate of increase of the supersaturation does lead to more controlled growth and crystals with better morphology. This effect is further mitigated by the presence of growing crystals or a precipitate both of which will act to lower the overall supersaturation. The slow rate of supersaturation can be achieved by using vapor diffusion equilibration in small diameter capillaries. An alternative approach which is potentially more controllable is to use the method proposed by Wilson and co-workers[8] in which flowing nitrogen of controlled humidity controls the rate of evaporation.

The ICL growth experiments conducted in the capillaries indicate that some convective mixing is beneficial to the crystal growth by providing mixing and a uniform supersaturation in the crystallizing solution. Pusey and co-workers[9] have demonstrated in the case of lysozyme that high flow rates can cause cessation of growth. However, most small molecule aqueous crystal growth is done with some form of stirring (see i.e. Buckley[10] and Chernov[1]). The best crystals will be expected to be found between the extremes of no flow (mixing) and rapid flows which can cause cessation of growth in protein systems.

The usual flows found in protein crystallization are due to solutal convection where gravity acts on density differences at the growth interface or at the vapor-liquid interface where evaporation is taking place. These flows can be non-uniform and unpredictable. The capillary experiments with ICL may have been fortuitous in that the size of the capillary and the volume of solution may have provided a Grashof number which yielded a suitable flow regime for growth. It is possible to engineer growth systems to give the proper Grashof number if the parameters of the system are known. However, the need to quantify the parameters can be by-passed by using gravity as a variable. To date this parameter has been explored only at the limits available: 1-g and μg. Experiments in an induced artificial gravity between the extremes are needed to study the effect of gravity and flow on the growth and morphology of protein crystals.

While the lack of fluid flow in a μg environment is a factor in the improved quality of space grown ICL crystals. The results of this study indicate that lack of fluid flow around the crystal may not be as important factor as the lack of mixing in the drop itself. This lack of mixing in the drop allows the protein to precipitate at the liquid-vapor interface thereby lowering the supersaturation at which the crystal grows. This lowered supersaturation leads to a slower growth rate which improves the crystal morphology.

More study is needed both in 1-g and μg to determine if this mechanism is operative in other protein systems.

III. CONTROL OF NUCLEATION

It is well known that crystal growth involves two separate processes; 1) nucleation of the species desired, and 2) the growth of these nuclei into macroscopic crystals of suitable size and quality for the intended application. Nucleation involves a phase transformation in which a solid surface of the phase desired is created within a nutrient phase. The crystal growth process, on the other hand, involves heat and mass transport, i.e. removing the latent heat evolved during the crystallization process and supplying nutrient to the growing crystal at an appropriate rate. It is not surprising, therefore, that the energetics involved in these two processes are not the same. In many cases, they are significantly different.

It is of practical importance to be able to isolate and control the nucleation process separately from the subsequent growth phase. In small molecule crystal growth, this is most often accomplished by introducing an appropriate seed crystal (usually of the material being grown) into a melt, vapor, or solution. The use of a seed by-passes the nucleation stage by providing the solid-liquid interface necessary for the crystal growth process to proceed. In the growth of crystals containing biological macromolecules, obtaining seeds of the appropriate size and quality is often very difficult and has rarely been an attractive strategy. In most macromolecular crystal growth processes currently in use, the nucleation step is achieved in the growth solution under poorly understood conditions and the growth proceeds in a more or less uncontrolled manner.

In crystal growth from aqueous solutions, (the principal, if not only method, for growing crystals of biological species) the driving force of nucleation is the supersaturation. The supersaturation, c/s, where c is the actual solution concentration and s is the concentration at the saturation point, provides the excess energy needed to form the solid surface in the solution phase (homogeneous nucleation). The temperature-composition diagram in Fig. 9. illustrates the relationship between solubility and supersaturation. The solid line is the solubility curve, which divides the diagram into two regions: unsaturated and supersaturated. A second curve, the supersolubility curve, divides supersaturated region into labile and metastable regions. The labile region is unstable and nuclei form readily by spontaneous fluctuations in composition. Solutions are quite stable in the metastable state and it is only in this region where controlled crystal growth is possible.[1] The width of the metastable region depends on a number of factors, including purity of the starting materials. The supersaturation needed for homogeneous nucleation is often significantly greater than that needed for growth and that is why, after the initial nuclei are formed, growth normally proceeds in a rapid uncontrolled

manner. The supersaturation necessary for nucleation can often be reduced if a foreign substance is present upon which the species of interest prefers to nucleate (heterogeneous nucleation).

Starting from an undersaturated condition, the metastable region can be reached in principle by either changing temperature at constant composition or composition at constant temperature. Most biological macromolecular crystals are grown by the latter technique because the temperature dependent coefficient of solubility (phase equilibria) is usually not known and, in some cases, is negligible.

With respect to both nucleation and growth processes, temperature change methods are usually easier to control with more precision than other techniques such as evaporation and therefore, if possible, would be the method of choice.

One method for controlling nucleation without using seeds involves the localized control of supersaturation in a specific region of a near-saturated bulk solution. By doing so, nucleation will be confined to a small volume of the solution and the number of crystallites which form will thus be severely limited. With the bulk of the solution near or just at saturation, the crystals nucleated can then be grown in a controlled manner by changing the solution temperature and hence the bulk supersaturation.

Localized nucleation can be accomplished by controlling temperature or solute concentration in that region. The Thermonucleator was designed to accomplish this and controls the localized supersaturation by controlling the temperature in an approximately 0.4 mm^3 region of a >1 cm^3 protein solution. The steep temperature gradients developed can therefore restrict nucleation to a very small volume of the overall solution. An illustration of the process is given in Fig. 10.

The Thermonucleator controls both the cold spot temperature (T_S) and the ambient temperature around the growth cell (T_e). The procedure for nucleating a desired crystal is generally as follows: 1) The bulk solution is set at a near saturation (Fig. 10a). Under these stable conditions, critical size nuclei should not form. 2) T_S is adjusted so that the supersaturation is large enough to cause nucleation on the exposed surface of the cold finger (Fig.10b). The amount of undercooling should be such that the surface of the copper is at a temperature just inside the labile region described in Fig. 9. If the phase equilibria data (solubility) is not known, it is a rather simple matter to empirically find the appropriate temperature to cause nucleation to take place on the cold finger. 3) After solid forms on the tip, T_S (and sometimes T_e) is raised to try and dissolve all but a few of the crystallites which may form initially. In practice, this is difficult to achieve because it is hard to see very small crystallites in the growth cell. Laser light scattering techniques, when developed and incorporated into the system, should provide more control of this

process. 4) After dissolving back the initial crystallites, T_S is decreased to that of the bulk solution, and 5) The temperature of both the bulk solution and the tip are slowly lowered to cause growth to take place on the existing seed or seeds (Fig. 10c). This proceedure has been used to successfully grow crystals of ice, Rochelle salt and lysozyme.

Figure 11 illustrates a problem that was encountered with the nucleation of lysozyme. Though the initial stages of crystallization seemed to show only a few nuclei, the growth rapidly became polycrystalline. In a subsequent crystallization a different approach was employed. The bulk temperature (T_e) was set at 22°C and the cold finger temperature (T_S) at 12°C. After 6.5 hrs, crystals appeared on the cold finger (Fig. 12) and T_e and T_S were adjusted to 20°C. Observation after an additional growth period of 15.5 hrs showed that there was a polycrystalline mass on the cold finger. The temperatures were raised (T_S to 28°C and T_e to 26°C) to dissolve all but a few of the crystals. When only a few crystals remained (after 7.5 hrs), the temperatures were lowered to continue the growth (T_e=21°C, T_S=20°C). The temperatures were lowered 2°C increments over the next few days as growth continued. The final temperatures were T_e =18°C and T_S =16°C. During this growth sequence (Fig. 12), one large (270μ) crystal and several smaller crystals were formed on the cold finger.

The ideal in the nucleation process is to halt the nucleation process when the first nucleus is formed and to begin the growth phase of the crystal growth process. Careful visual observation can reveal the presence of nuclei in the 10μm range and was used to grow the crystal shown in Fig. 13. Using the visual approach requires some knowledge of the time required for nucleation. Since this information is not always available and visual inspection is not possible under μg conditions, techniques are under study to detect nucleation using light scattering.

Not all proteins exhibit normal solubility (increase of solubility with increasing temperature), some, including lysozyme above 30°C, horse serum albumin and α Chymotrypsinogen A, are less soluble as the temperature increases (retrograde solubility). Lysozyme crystals were nucleated above 30°C (Fig. 14) to demonstrate the Thermonucleator's ability to nucleate proteins with retrograde solubility. This was also a demonstration of the use of the Thermonucleator to nucleate crystals without a prior knowledge of the solubility curve, since the solubility curve of lysozyme above 30°C is not known. Convection was noted above the nucleating tip, but there is a region of no flow immediately adjacent to the surface of the tip which allowed nucleation to occur. This thermally driven convection would not occur in μg.

The current version of the thermonucleator was built as a demonstration prototype both to test the feasibility of the concept and to provide a test bed for various monitoring

schemes. The size of the apparatus (15in x 13in x 19in), and its use of liquid nitrogen and water baths for temperature control mitigate against its use in μg in its present form. The proposed design for a more space ready prototype is shown in Fig. 15. This unit will use thermoelectric heating and cooling. The diagrams show water cooling being used to heat sink the thermoelectric elements. This is a matter of convenience and can be replaced by air cooled heat sinks. The growth cell is identical to that used in the current thermonucleator. The cell is surrounded by a 0.25in temperature controlled annulus formed by 4 flat optical windows to allow observation. The temperatures are sensed by thermistors in the annulus and in contact with the cold spot (not shown in fig.15). The temperatures are electronically controlled. This new version of the thermonucleator is presently under construction.

IV. REFERENCES

1. A. A. Chernov, Modern Crystallography III, Springer-Verlag, Berlin, 1984.

2. R.-F. Xiao, J. I. D. Alexander and F. Rosenberger, private communication.

3. L. Sibille and J. K. Baird, *J. Crystal Growth* 110 (1991) 72.

4. L. Sibille, J. C. Clunie and J. K. Baird, *J. Crystal Growth* 110 (1991) 80.

5. D. P. Shoemaker and C. W. Garland, Experiments in Physical Chemistry, McGraw-Hill, New York, 1962.

6. M. Pusey, private communication.

7. M. Pusey and R. Naumann, *J. Crystal Growth* 76 (1986) 593.

8. L. J. Wilson, T. L. Bray and F. L. Suddath, *J. Crystal Growth* 110 (1991) 142.

9. M. Pusey, W.K. Witherow and R. Naumann, *J. Crystal Growth* 90 (1988) 105.

10. H.E. Buckley, Crystal Growth, John Wiley and Sons, New York, 1951.

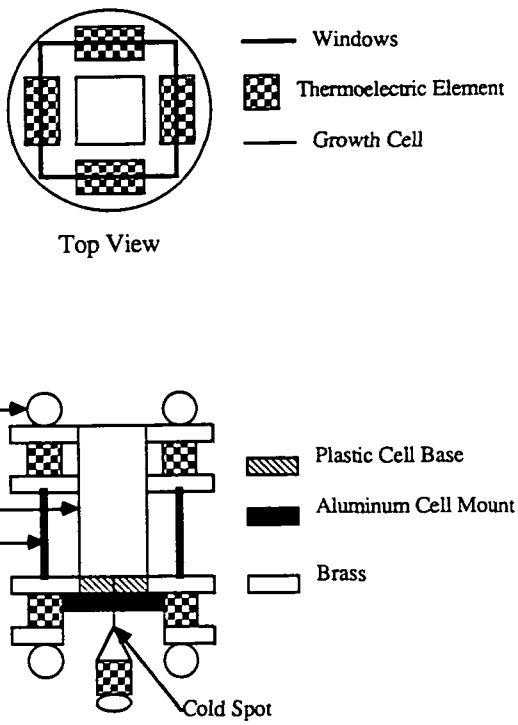

Fig. 15. Schematic of new thermonucleator prototype. Approximately full size.

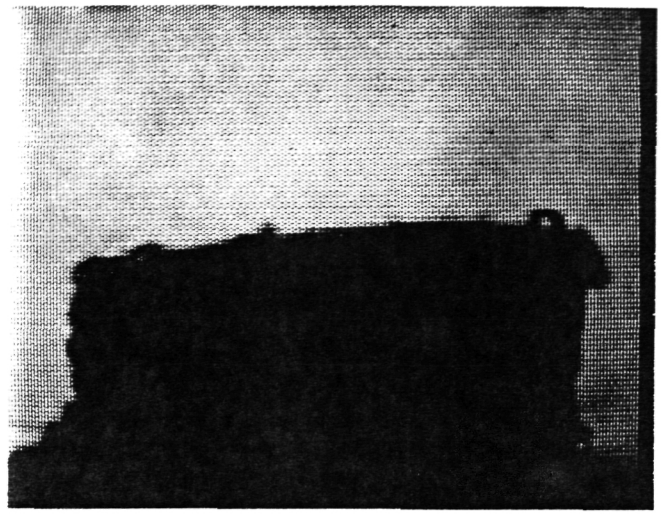

Fig. 13. A few small lysozyme crystals on the thermonucleator cold spot. Nucleation was stopped as soon as nuclei were vivible. Largest crystal is 40μm.

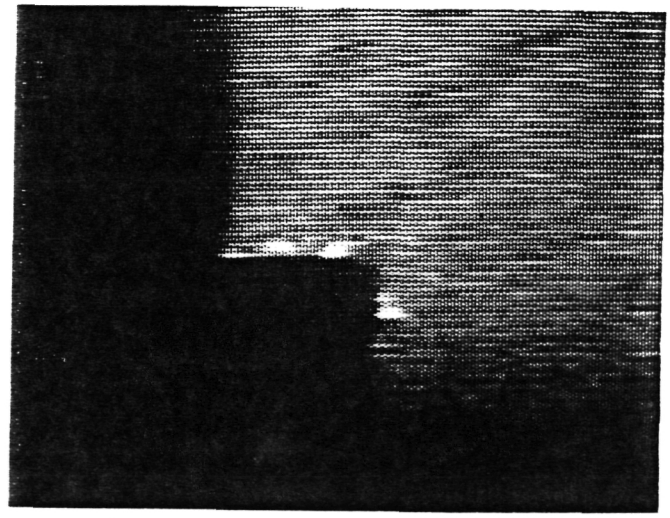

Fig. 14. Lysozyme crystals nucleated in the retrograde solubility regime.

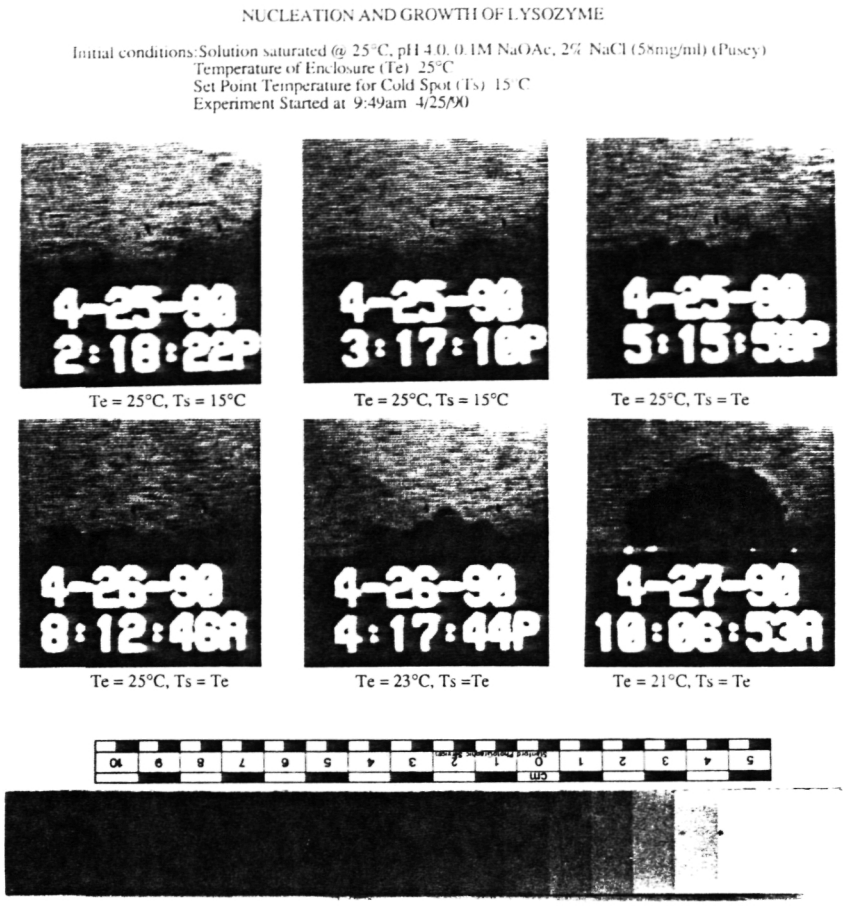

Fig. 11 Growth of lysozyme in thermonucleator. Growth starts with a few nuclei and progresses to a polycrystalline mass.

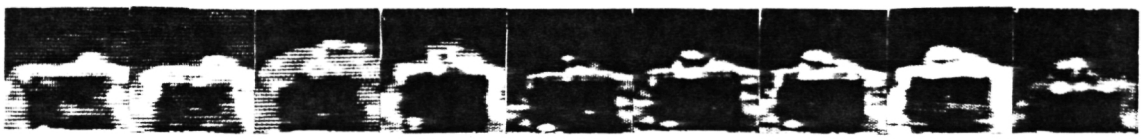

Date	7-24	7-24	7-25	7-25	7-25	7-26	7-29	8-1	8-5
Time	1002	1309	0804	1217	1435	1639	1433	1622	0757
Elapsed Time (hrs)	0	3.12	20.02	24.24	26.54	52.31	119.21	193.03	280.61
Spot Temperature (^{2}C) (c/s)	28 (.53)	12 (4.02)	22 (1.15)	28 (.53)	20 (1.50)	20 (1.50)	18 (1.98)	18 (1.98)	16 (2.57)
Ambient Temperature (^{2}C) (c/s	28 (.53)	22 (1.15)	20 (1.50)	26 (.66)	21 (1.31)	20 (1.50)	20 (1.50)	20 (1.50)	18 (1.98)
Size (μ)					147	191	221	269	269

Fig. 12. Photographs showing the results of the improved growth procedure for the growth of lysozyme.

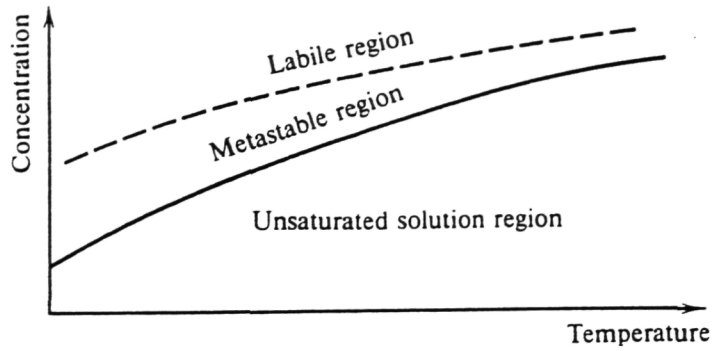

Fig. 9. Schematic diagram of solubility for a substance whose solubility increases with temperature.

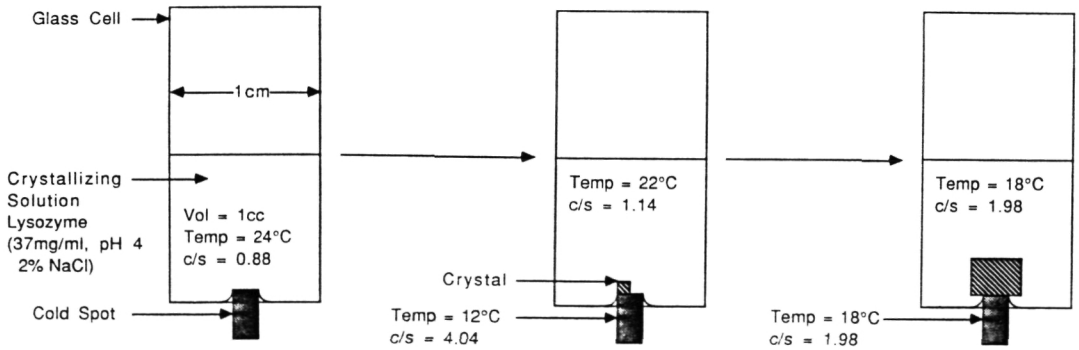

Fig. 10. Controlled nucleation using temperature control method (thermonucleation).

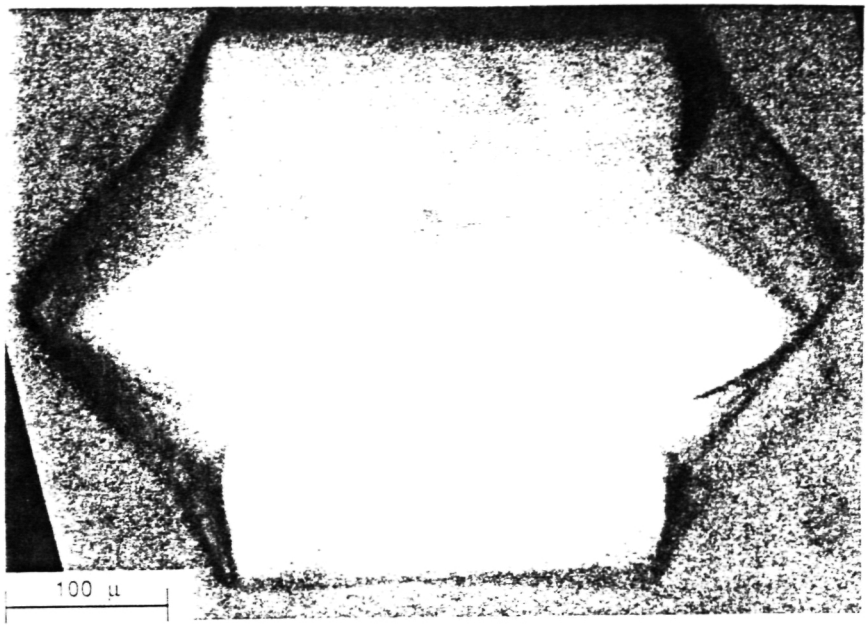

Fig. 7. ICL crystal grown from 30µl drop (10mg/ml) in µg.

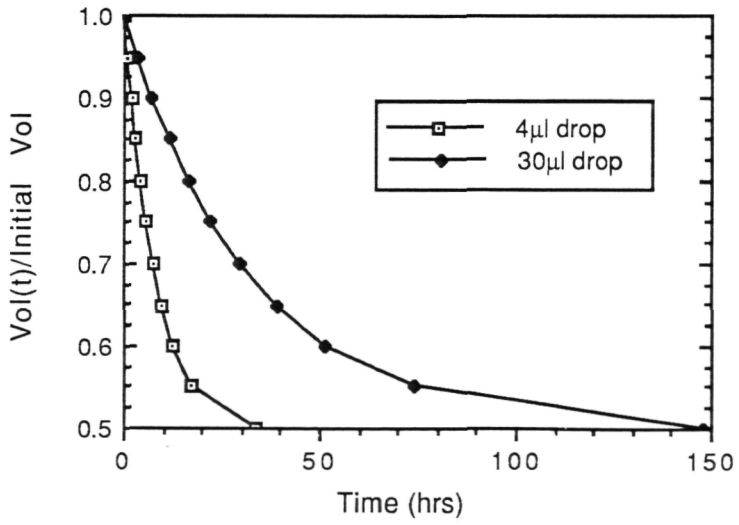

Fig. 8. Volume ratio vs. time comparing 4µl drop with a 30µl drop. Simulates ICL growth.

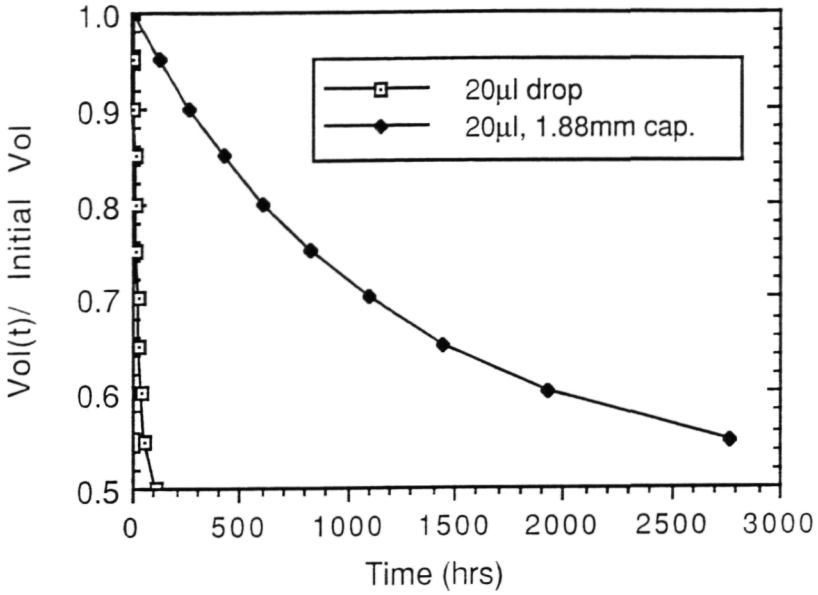

Fig. 5. Volume ratio vs. time comparing 20µl drop with 20µl in a 1.88mm capillary. Simulates ICL crystallization.

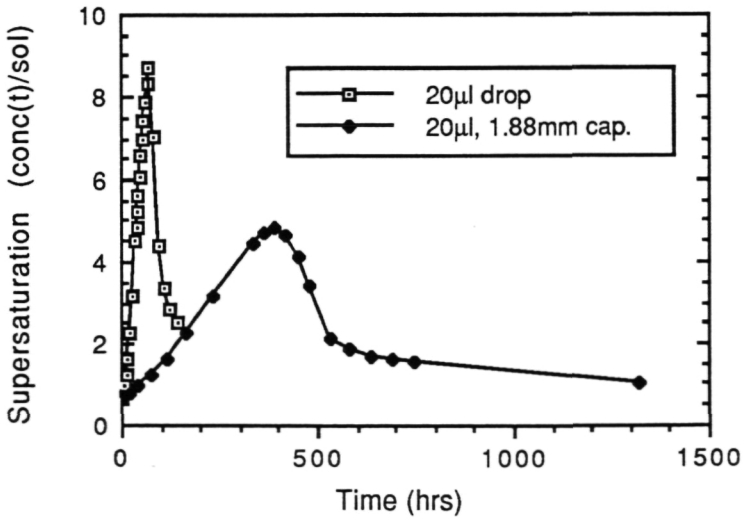

Fig. 6. Supersaturation vs. time for lysozyme comparing 20µl drop with 20µl in 1.88mm capillary. 10 crystals are nucleated at c/s = 4 and allowed to grow.

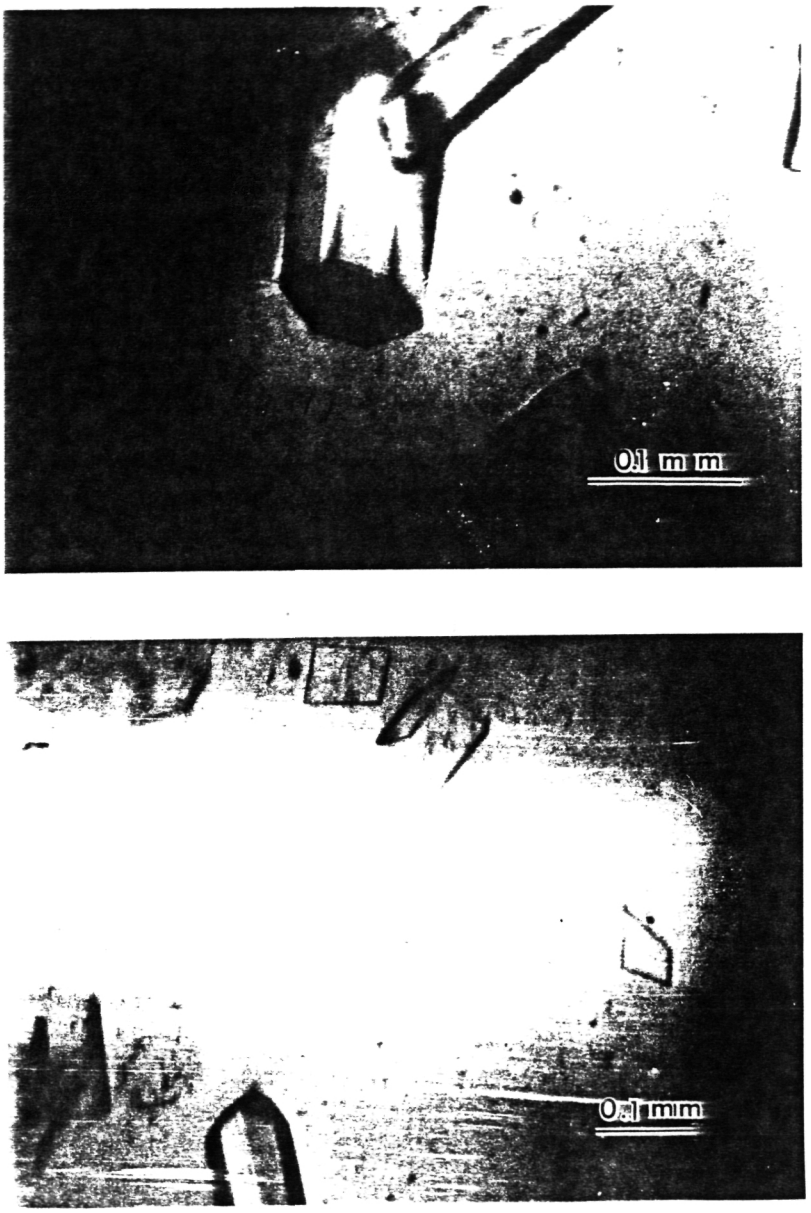

Fig. 4. ICL crystals grown in 1.88mm capillary (12mg/ml) showing a) flat termination by a (001) type face, and
b) a wedged shaped termination by (101) type face.

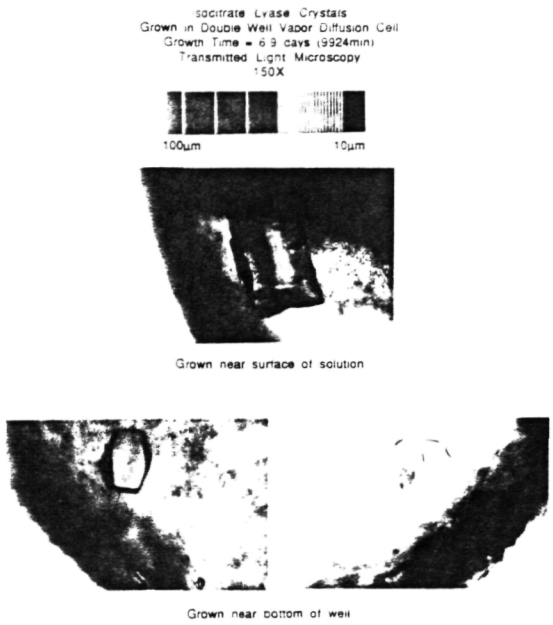

Fig. 3. ICL crystals grown in 1mm x 3mm cell (4µl of 12mg/ml).

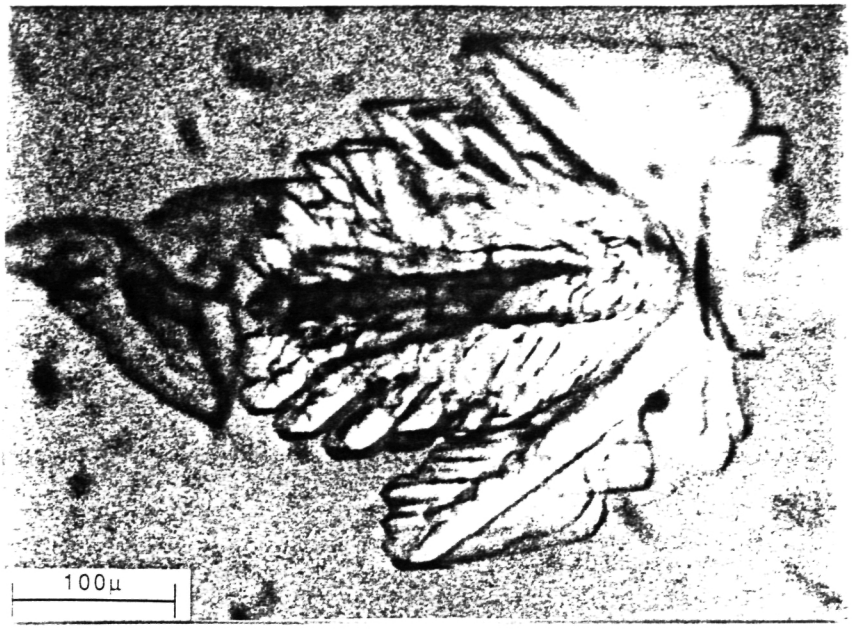

Fig. 1. Isocitrate lyase crystal (ICL) grown from 30µl hanging drop (ICL concentration 10mg/ml).

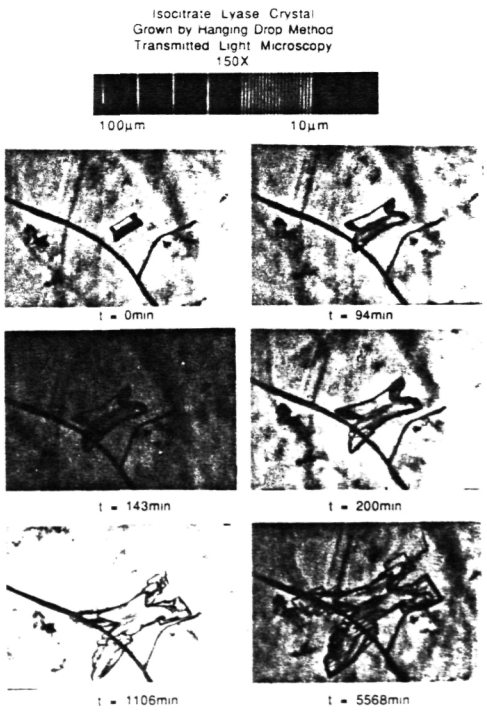

Fig. 2. Time lapse of ICL crystal grown from 4µl hanging drop (ICL concentration 12mg/ml).